PCCP

Accepted Manuscript

ROYAL SOCIETY OF CHEMISTRY

www.rsc.org/pccp

Singularities on the physicochemical properties of spontaneous AOT-BHD unilamellar vesicles in comparison with DOPC vesicles

Cristian C. Villa, N. Mariano Correa, Juana J. Silber, Fernando Moyano* and R. Darío Falcone*

Departamento de Química. Universidad Nacional de Río Cuarto. Agencia Postal # 3. C.P. X5804BYA Río Cuarto. ARGENTINA.

[*] Dr. Fernando Moyano. Corresponding-Author, E-mail: fmoyano@exa.unrc.edu.ar

Dr. R. Darío Falcone. Corresponding-Author, E-mail: rfalcone@exa.unrc.edu.ar

A**bstract**

In the present work we study different physicochemical properties of the spontaneous unilamellar vesicles created by the catanionic ionic liquids-like surfactant benzyl-n-hexadecyldimethylammonium 1,4-bis-2-ethylhexylsulfosuccinate (AOT-BHD), using two different fluorescent probes: 6-propionyl-2-(dimethylaminonaphthalene), PRODAN and trans-4-[4-(dimethylamino)-styryl]-1-methylpyridinium iodide, HC.

Steady-state and time resolved fluorescence emission spectroscopy allowed us to find unique properties on the AOT-BHD bilayer in comparison with vesicles formed with the traditional phospholipid 1,2-dioleoyl-sn-glycero-3-phosphocholine, DOPC. From the emission results, we observed that the region of the bilayer close to the polar head of AOT-BHD is a powerful electron donor environment, even larger than DOPC. Additionally, the AOT-BHD bilayer offers a less polar and slightly more viscous zone than the DOPC one.

Thus, this particular bilayer is able to produce large incorporation of ionic and nonionic molecules and is very promising to be used as nanocarrier in pharmacologic, cosmetic and foods fields.

Keywords: Catanionic surfactant, unilamellar vesicles, AOT-BHD, ionic liquid, HC, PRODAN.

Introduction

The cell membranes of almost all living organisms and many viruses are made of a lipid bilayer.[1-4] They serve as the platforms on which membrane proteins are localized and play a central role in a host of physiological processes.[1,4] As membrane-mimetic systems normally simpler systems are employed to study different properties.[5] Organized supramolecular assemblies, such as vesicles or liposomes, can be considered as large cooperative entities with very different characteristics from the individual structural units which constitute them.[6] Vesicles and liposomes are spherical aggregates formed by some amphiphilic compounds where the lipid bilayer surrounds an aqueous void volume which can be "loaded" with almost any variety of water-soluble marker molecules.[7-9] In order to prepare large unilamellar vesicles (LUVs) it is mandatory the use of different techniques (such as ultra-sonication or extrusion) to convert multilamellar vesicles (formed spontaneously) into LUVs.[8,10,11] There are a wide kind of surfactants that form vesicles and, probably the most frequently used are the phospholipids, specially the phosphatidylcholine series[7] since these surfactants are the fundamental matrix of natural membranes and represent the environment in which many proteins and enzymes display their activity.[1,3,4] Additionally, the vesicles formed by phospholipids can enhance drug stability, therapeutic effects, and uptake of the solubilized drug into the target site with reduced toxicity.[12] Nevertheless, the stability of this kind of vesicles under extreme conditions is still a challenge and consequently its use as nanocarriers is limited. Hence, the research of alternative vesicles has recently been increased.[13-16]

It is known that the mixtures of surfactants can exhibit considerable synergistic advantages in their properties and application.[17,18] In this sense a new class of surfactant emerges: the *catanionic surfactants*.[19-30] They can be classified into two categories: i) The mixed surfactants counterions are present in the final system and the studies are performed in water. For example, Kaler et al.[31] reported the first vesicles (known as catanionic vesicles)

formed by mixing sodium dodecylbenzenesulfonate and cetyltrimethylammonium tosylate without removing the conterions and these can not be used in nonpolar solvents because the presence of the salt formed by the counterions. ii) The second category corresponds to the true catanionic systems when surfactants are mixed and the counterions are removed.[20-22] This category can also be divided into two subgroups: a) Surfactants that are obtained from their acid or hydroxide forms and no salt from the initial counterions is present. For example: the typical mixtures of alkyltrimethylammonium hydroxide and fatty acids where the counterions of the surfactants recombine to form water.[23-29] These kind of salt-free catanionic surfactants were investigated generating them *in situ* and no attempts to isolate the resulting surfactants were done. b) The other group of true catanionic surfactants emerge when ionic surfactants (not the one included in group (a)) are mixed in a 1:1 ratio and the inorganic salt is totally removed.[30] Particularly, some these surfactants[32,33] showed a rich thermotropic behavior, in some cases having 4 different mesophases between solid and liquid. The catanionic surfactants (group b) are attractive[30] because they have shown the ability to form different organized systems such as: normal and reverse micelles (RMs)[22,30-40], vesicles[22,36-41] and liquid crystals.[36-40,42]

Another attractive topic is the emerging field where ionic liquids[43-48] (ILs) with amphiphilic properties are synthesized.[49-53] In this sense, recently[22,40], we reported the synthesis of a new catanionic IL-like surfactant benzyl-n-hexadecyldimethylammonium 1,4-bis-2-ethylhexylsulfosuccinate, AOT-BHD (Scheme 1), resulting from the mixture of sodium 1,4-bis-2-ethylhexylsulfosuccinate (Na-AOT) and benzyl-n-hexadecyldimethylammonium chloride (BHDC), which showed characteristics of a room temperature IL with amphiphilic properties. This IL-like surfactant was isolated from the original surfactant mixture (removing the Na^+ and Cl^- counterions) and showed properties absolutely different from Na-AOT and BHDC. Particularly, we demonstrated that this unique surfactant can form both different

organized systems (RMs and vesicles) depending on the solvent used. Thus, we investigated its ability to form RMs in nonpolar solvents[22,40] and spontaneous LUVs in water[22] that are not in equilibrium with multilamellar ones. As AOT-BHD is probably the first synthesized IL-like surfactant that does not involve energy to form LUVs, it is very important to know the physicochemical properties (such as micropolarity, microviscosity or electron donor ability) of the AOT-BHD bilayer formed in water, if this new organized system want to be used as drug delivery agent.[12] Thus, in order to acquire valuable information about the AOT-BHD vesicles, we have choose two different fluorescent probes: 6-propionyl-2-(dimethylaminonaphthalene), PRODAN (Scheme 1) and, trans-4-[4-(dimethylamino)-styryl]-1-methylpyridinium iodide, HC (Scheme 1), which can sense different physicochemical properties of their microenvironment.[54-70]

PRODAN, has been the subject of many studies in the last two decades due to its high sensitivity to the environment, which makes it useful as a fluorescent probe for different kind of organized media.[59-61] In this sense, it is a fluorescent probe that emits an intense, single broad fluorescence band, strongly red-shifted with increasing the polarity-polarizability (π^*) and the hydrogen donor ability (α) of the media.[57,59,61,68-73]

HC is a molecular probe with a particular photophysical behavior,[58] which shows an absorption band that shifts to higher energy while, the emission band shifts to lower energy when the polarity of the media increase. These properties were assigned to the intramolecular charge transfer (C.T.) process in the excited state and to different interactions of the ground and C.T. states with the environment. Thus, the asymmetrical solvatochromism was explained considering that the excitation starts from a ground state where the positive charge is located mainly on the pyridinium ring and, the emission decay from an excited state, where the positive charge is mainly on the aniline ring (C.T. in Scheme 2).[56] Additionally, HC undergoes specific interactions with solvents that present electron donor ability (β solvent

parameter[54,56]). Thus, the absorption band shifts bathocromically with β increase while, the emission band shifts hypsochromically.[58] It seems that the positive charge located at the pyridinium ring of the HC in the ground state interacts with the electrons in a different way than the positive charge located in the aromatic dialkylamino group in the C.T. excited state (Scheme 2). On the other hand, HC tends to aggregate or cannot be dissolved in solvents where the β parameter is null or low.[58] In this sense, we have demonstrated that in organized systems such as BHDC RMs, HC can be dissolved perfectly and emits from another emission state, different to the C.T. state, where the positive charge is not delocalized in a preferred region, the L.E. state (see Scheme 2). This emission state is very less sensitive to the microenviroment than the C.T. state.[54,56]

Taking into account knowledge about PRODAN and HC as molecular probes, in the present work we show results obtained in AOT-BHD vesicles using steady-state and time resolved fluorescence emission spectroscopy. As comparison we also show results reported for DOPC vesicles, in order to elucidate similarities and differences between both vesicles that can be very valuable for future applications of the new system.

Results and Discussion

In order to present our results more clearly we have divided the work into two sections. In the first section, we show the data obtained using HC as a molecular probe in the AOT-BHD vesicles and in the second part, we report results obtained using PRODAN as probe. In both systems studied, the surfactant concentration was varied from 0 to 5 mg/mL; maintaining constant the molecular probe concentration. HC and PRODAN were used at $1x10^{-5}$ M and $5x10^{-6}$ M respectively since both dyes are fully solubilized as monomers at these concentrations.[54,57]

1. HC in AOT-BHD vesicles

The HC absorption maximum band shifts to the blue only 3 nm when the surfactant concentration increases (See absorption spectra of HC as a function of [AOT-BHD] in Figure S1, supporting information section). Since the most important changes are observed from emission spectroscopy, we will show and discuss only the emission data. Figure 1 shows the emission spectra of HC obtained in AOT-BHD vesicles varying the surfactant concentration. As [AOT-BHD] increases two results can be highlighted: i) HC emission intensity increases noticeably and, ii) the maximum emission band shifts hypsochromically. In order to explain these results, two facts of the particular HC´s behavior must be taking into account.

As the HC emission fluorescence is strongly inhibited in bulk water,[74] the enhancement of the HC emission intensity when increases AOT-BHD concentration, could suggests that the probe is incorporate from water to AOT-BHD vesicle, probably into the bilayer.

In Figure 2 is plotted the HC emission maxima varying the AOT-BHD concentration and it is observed that there is notorious blue shift (33 nm in comparison with the emission in pure water, λ_{em} = 615 nm) in the emission band until concentration around 2 mg/mL, after that the maximum band remain practically constant. The result can be explained as follow: Initially, at [AOT-BHD] = 0, HC in water undergoes a C.T. process in the excited state (see Scheme 2), where the charge is mainly localized on the ammonium group of HC. When the surfactant concentration increases, HC partitions from bulk water to the AOT-BHD bilayer (a less polar region than water), thus the large hypsocromic shift observed in AOT-BHD vesicles suggest two facts: i) HC sense a less polar environment upon [surfactant] increases due to its incorporation into the bilayer and, ii) upon exciting, HC has the positive charge located on the ammonium group (C.T. sate) which could interact with the electron donor region of the AOT-BHD bilayer. Thus, when HC is incorporated to the bilayer sense a more electron donor

microenvironment because the HC positive charge is near the succinate group of surfactant AOT-BHD, which is a region with large electron donor ability[54,56] that can stabilize the C.T. specie.

The behavior of HC in DOPC LUV using static and time resolved emission spectroscopies was also studied by our group.[58] In Figure 2, is included for comparison the results obtained for HC in DOPC vesicles. As can be observed there are differences in the HC emission maximum band in AOT-BHD in comparison with the results reported in DOPC vesicles.[58] For example, at [surfactant] = 2 mg/mL in AOT-BHD vesicles the blue shift is 33 nm while to DOPC vesicles is 18 nm with respect to the pure water. At [surfactant] ≥ 2 mg/mL the maximum band remain practically constant in both systems. Thus, at [surfactant] = 2 mg/mL, the emission maxima of HC peaks at λ_{max}= 582 nm in AOT-BHD vesicles and at λ_{max}= 597 nm in DOPC vesicles. These suggest a different environment sensed by HC in both vesicles. Therefore, HC senses a more electron donor and less polar environment in AOT-BHD than in DOPC vesicles.

In order to get more information about the properties of the AOT-BHD bilayer such as micropolarity, microviscosity, capacity of donor electrons and different regions into bilayer to compare with the DOPC one, we performed two different wavelength–selective fluorescence approaches such as: red–edge excitation shift study (REES) and fluorescence lifetimes.[57,58]

In general, for fluorophores in a bulk non-viscous solvent, the dipolar relaxation of the solvent molecules around it in the excited state is much faster than fluorescence decay.[75] Hence, the wavelength of maximum emission usually is independent of the excitation wavelength.[75] However, excitation wavelength dependence is observed if the dipolar relaxation time of the solvent molecules is comparable to or longer than the fluorescence lifetime.[75] Thus, a shift in the emission maximum wavelength toward higher values, caused by a shift in the excitation wavelength toward the red edge of the absorption band, is known

as the red edge excitation shift (REES).[75,76] This approach can be used to directly monitor the microenvironment and dynamics around a fluorophore in a motion restricted media such as reverse micelles or vesicles.[6,56-58,77,78]

1.1 Red–Edge Excitation Shift Study (REES)

Figure 3 shows the shift in the maxima of the HC emission fluorescence in both AOT-BHD and DOPC vesicles as a function of the excitation wavelength at different surfactant concentrations, being REES = $\Delta\lambda_{em}$ = ($\lambda_{em\ (exc\ 510nm)}$ - ($\lambda_{em\ (exc\ 450nm)}$). The results show that as the AOT-BHD concentration increases, the magnitude of the HC's REES also increases noticeably up to [AOT-BHD] ~ 2 mg/mL. At this catanionic surfactant concentration the value sensed by HC is around 11 nm, which shows that HC molecule senses a motion constrained environment (the AOT-BHD bilayer) in comparison with the water pseudophase (REES = 0). On the other hand, HC senses a REES value of 9 nm for the same surfactant concentration in DOPC vesicles.[58] Even that the difference between both values is not large is possible to conclude that HC senses a slightly more viscous environment in AOT-BHD than in DOPC. Apparently, the bilayer composed by both amphiphilic moieties, the anionic AOT and the cationic BHD, make the bilayer slight more rigid than the phospholipid one. This difference in rigidity can be suggesting a different water penetration into the bilayer (less water penetration in the AOT-BHD bilayer, more rigidity).

1.2 Fluorescence Lifetimes

In addition to the REES experiments, fluorescence lifetimes (τ) are also dependent on the excitation and emission wavelengths in viscous solution and in otherwise motion restricted media.[75] Thus, τ serves as sensitive indicator for the local microenvironment where

a solute exists because differential extent of solvent relaxation around a given fluorophore could be expected to give rise to differences in its fluorescence lifetime.[57,58,75,78]

In bulk water the HC's fluorescence lifetime value is 11 ps.[58] However, the situation is different when the HC is incorporated into bilayer in AOT-BHD vesicles. For example, in Figure S2 (supporting information section) the emission decay for HC in AOT-BHD vesicles at [AOT-BHD] = 2 mg/mL is shown. Table 1 shows the fluorescence lifetime of HC in AOT-BHD at different emission wavelengths and [AOT-BHD] = 2 mg/mL. In Figure 4 is plotted for comparison the fluorescence lifetime values for HC in AOT-BHD and DOPC vesicles. As it can be seen from Table 1, the emission decays fits nicely to a single exponential function at any wavelength. From Table 1 and Figure 4 is possible to observe that the HC´s τ values increases when the emission wavelength increases, they are different in both vesicles and larger than in bulk water.

The fluorescence lifetimes increment as the emission wavelengths change from 585 to 645 nm (the red edge of the emission band) suggests than that fluorophore is located in environments of restricted mobility.[75,79] If HC would be located near the water side, no dependence with the emission wavelength should be observed. Indeed, HC is sensitive enough to monitor the bilayer dynamics and the electron rich environment and it is due to the fact that the positive charge of the HC molecule is maybe close to the succinate group of the AOT-BHD inside the bilayer.

On the other hand, HC presents larger fluorescent lifetime ($\tau \sim 1.5$ ns) in AOT-BHD vesicles than in DOPC ($\tau \sim 0.5$ ns). These differences may be ascribed to different microenvironments surrounding to HC in each bilayer. We demonstrated[58] that in DOPC vesicles HC interacts with the phosphate group of the phospholipid at the interface and due to the proximity of the water molecules causes an inhibition of the emission of HC and therefore shorter fluorescent lifetimes. In AOT-BHD vesicles, HC interacts with the succinate group of

the AOT-BHD but water is far away from this region and consequently less inhibition of the HC emission and, fluorescent lifetime larger are observed. These facts demonstrate that the water molecules penetrate less in the AOT-BHD than DOPC bilayer as it was suggested from the REES values. In Scheme 3 is shown the possible location of HC and the water molecules in both AOT-BHD and DOPC vesicles.

2. PRODAN in AOT-BHD vesicles

Since the absorption band (See Figure S3 in supporting information section) does not show significant changes (the maximum band peaks at λ_{max} = 355 nm) when the [AOT-BHD] increases we only discuss the results obtained from the emission band. Figure 5 shows typical emission spectra of PRODAN at different [AOT-BHD]. When the [AOT-BHD] increases, the band around λ = 525 nm, which correspond to PRODAN in water, disappear and a new band emerges around λ = 450 nm. When the [AOT-BHD] is larger than 2 mg/mL only a single band appears at λ_{max} = 448 nm. The hypsochromic shift of the emission band indicates that PRODAN sense a less polar environment.[57] As it can be observed, at high [AOT-BHD] ($\geq$ 2 mg/mL) the emission band appears practically symmetrical, suggesting that PRODAN is located in one region of the bilayer. Different behavior was observed for PRODAN in DOPC vesicles.[57] We found that at [DOPC] > 1 mg/mL PRODAN is completely incorporated into the bilayer of DOPC but senses two different microenvironments: a polar region near to the interface with a maximum at λ = 494 nm and a less polar environment with a shoulder at λ = 430 nm. Taking into account that PRODAN maximum emission at [AOT-BHD] > 1.5 mg/mL appears at λ = 448 nm, we conclude that inside the bilayer PRODAN senses a less polar environment compared to DOPC vesicles.

2.1 Red–Edge Excitation Shift Study (REES).

Figure 6 shows the shift in the PRODAN emission maxima in DOPC and AOT-BHD bilayers as a function of the excitation wavelength at different surfactants concentrations. The results show that as the AOT-BHD concentration increases, the magnitude of the REES also increases from 0 to 9 nm, remaining constant for [AOT-BHD] ≥ 2 mg/mL. These REES values suggest that PRODAN is located far away from the hydrocarbon tails (fluid microenvironment) and/or it is near to the polar head (less fluid microenvironment). If the REES values of PRODAN in AOT-BHD and DOPC vesicles are compared, different profiles are observed. From Figure 6, a gradual increment in the REES value is observed in AOT-BHD vesicles. However, in DOPC an initial increment of REES value was observed until [DOPC] around 0.5 mg/mL and then at higher [DOPC] a decrease in the value was detected. The particular behavior for PRODAN in DOPC vesicles was explained[57] that at low [DOPC] (< 1 mg/mL) the probe is partitioning between water and the bilayer[57] and, PRODAN inside the aggregate is located in a motionally restricted media comparing with the PRODAN molecules in water. At higher DOPC concentration, PRODAN is totally incorporated into the vesicle. Thus, using the model proposed by Chong[80] we suggested that, PRODAN incorporated into the bilayer can be suffering a partition from the polar environment (the viscous interfacial region with a peak around λ = 490 nm) into the less polar one with a less viscous microenvironment corresponding to the peak around λ = 430 nm. Comparing the AOT-BHD and DOPC results is possible to conclude that at [AOT-BHD] > 2 mg/mL the presence of only one peak at λ = 448 nm in Figure 5, indicates that only one PRODAN species is located inside the bilayer. In Scheme 4 is shown the probably location of PRODAN in both AOT-BHD and DOPC vesicles.

2.2 Fluorescence Lifetimes.

In Table 2 are gathered the fluorescence lifetime values of PRODAN varying the [AOT-BHD] at [PRODAN] = 5 x 10^{-6} M. Several interesting facts can be obtained depending on the AOT-BHD concentration. At [AOT-BHD] < 2 mg/mL and λ_{em} = 525 nm (λ_{exc} = 378 nm), the decay is biexponential with fluorescence lifetimes matching to the specie in the polar environment (PRODAN in water, $\tau_1 \approx 0.7$ ns) and the other species could be PRODAN inside bilayer, $\tau_2 \approx 3.8$ ns (non-polar microenvironment), evidencing a PRODAN partition process between water and the AOT-BHD bilayer. Note that when the [AOT-BHD] increases the percentage of the shorter τ (PRODAN in water) decreases with the consequent increasing on the proportion of the longer τ (PRODAN at the bilayer). Once the probe is totally incorporated into the bilayer ([AOT-BHD] > 2 mg/mL), it can be seen that the decay becomes mono-exponential with fluorescence lifetime values that match the one that correspond to the species in a non-polar environment.[57] On the other hand, as it was previously reported[57] PRODAN in DOPC vesicles even at higher [DOPC] showed bi-exponential decays which were explained considering two different regions in the DOPC bilayer (see Scheme 4).

As it was mentioned, when the catanionic surfactant concentration increases, both HC and PRODAN are incorporated from the bulk water to the AOT-BHD bilayer. This phenomenon can be very interesting if the AOT-BHD vesicles are wanted to be used as drugs deliveries agent, so is must be valuable to know how the magnitude of the partition constant is for these two molecules. To evaluate the partition constant, K_p, we use the changes in its emission spectra with the [AOT-BHD] (Figures 1 and 5) following a procedure used in other organized media.[57,58] For detailed procedure see Supporting Information section.

Determination of K_p

Figures S4 A and B show the increment of the probes fluorescence intensity when AOT-BHD concentration increases for HC and PRODAN taken from Figures 1 and 5,

respectively. As it can be observed in both Figures, the changes of the intensities on increasing the [AOT-BHD] are not linear for both probes. Moreover, the most important changes are observed until [AOT-BHD] around 2 mg/mL. These variations suggest that after that [AOT-BHD] the molecular probes are practically incorporated into the vesicle bilayer and no more changes are expected since the environment of the probe does not change. Thus, using a least-squares fit of equation S5 (supporting information section) we calculate the values of K_p for HC and PRODAN in AOT-BHD vesicles which are recorded in Table 3. Also, for comparison in the same Table are the corresponding values for both molecules probes in DOPC vesicles.[57,58]

As it can be observed from Table 3, HC shows different K_p values in both vesicles. Thus, the K_p value obtained for HC in AOT-BHD vesicles (18.9 mL/mg) is larger than that reported for DOPC (2.35 mL/mg).[58] The K_p value found for AOT-BHD, which is around 8 times larger than from DOPC, emphasize the idea proposed above that HC into the bilayer of AOT-BHD is located in a less polar region but also with more electron donor environment in comparison with DOPC.

For PRODAN, K_p values of 25 mL/mg in AOT-BHD and 16 mL/mg in DOPC[57] vesicles are obtained. The larger K_p value found in AOT-BHD indicates that PRODAN is more incorporated into the bilayer in comparison with the DOPC and this is probably because the bilayer provides a less polar region in comparison with DOPC.

Finally, our results show how structural differences (chemical structure of the surfactant and water penetration into the interface) in the bilayers of both vesicles influence strongly in the incorporation of two different kinds of molecules ionic and nonionic one. Thus, even that both molecular probes are located in different regions at the bilayer (see Schemes 3 and 4), the AOT-BHD vesicles allows a larger incorporation of ionic and nonionic solutes than the

DOPC vesicles, fact than can be essential to use these novel unilamellar vesicles as nanocarriers.

Conclusion

The behavior of two fluorescent probes (PRODAN and HC) were studied in the spontaneous large AOT-BHD LUVs, using emission and time resolved spectroscopies. Interesting different features of the AOT-BHD bilayer properties in comparison with DOPC were observed.

From the emission results, we demonstrated that the region of the bilayer close to the polar head of AOT-BHD is a powerful electron donor environment even larger than DOPC. In term of polarity, the AOT-BHD bilayer offers a less polar zone than the DOPC one. To monitor directly the dynamics around PRODAN and HC inside the AOT-BHD bilayer, we use the wavelength–selective fluorescence approach. The results show that the AOT-BHD bilayer is slightly viscous than the DOPC bilayer.

In summary, our results suggest that the AOT-BHD vesicles present a bilayer completely different to the DOPC one, with low polarity, high viscosity and more electron donor capacity. These properties produce large incorporation of ionic and nonionic molecules, which are very promising to use in a future this kind of organized media as nanocarrier in pharmacologic, cosmetic and foods fields.

Experimental section

Materials

The catanionic IL-like surfactant used, benzyl-n-hexadecyldimethylammonium 1,4-bis-2-ethylhexylsulfosuccinate (AOT-BHD, Scheme 1) was synthesized following our previous procedure described in reference 22 and, was dried under vacuum prior use.

Ultrapure water was used throughout and prepared to a specific resistivity of > 18 MΩ cm (Labonco equipment model 90901-01).

The fluorescent probe 6-propionyl-2-dimethylaminonaphthalene, PRODAN, from Molecular Probes (Eugene Or), was used without further purification. Trans-4-[4-(dimethylamino)-styryl]-1-methylpyridinium iodide (HC) was synthesized through a modification of method described in references 81 and 82.

Methods

The AOT-BHD vesicles solutions containing the molecular probes were prepared as follows: an appropriate amount of molecular probe stock solution in acetonitrile (Sintorgan HPLC grade) was transferred into the volumetric flask using a calibrated microsyringe. The solvent was evaporated by bubbling dry N_2, and the residue dissolved with pure water to obtain a final PRODAN or HC concentration of 5 x 10^{-6} M and 1 x 10^{-5} M, respectively. Then, these solutions were used as a solvent to dissolve an appropriate amount of AOT-BHD (by weight) in order to prepare the LUVs stock solutions of 5 mg/mL. The opalescent solutions obtained were shook about 2 minutes at room temperature.

In the AOT-BHD dilution experiments, the samples composed of both, the surfactant AOT-BHD and the probe were diluted by adding probe water solution. To subtract the background contribution for the absorption and emission experiments, samples of the AOT-BHD surfactant at the same concentrations were prepared, omitting the addition of the probe. All samples were prepared and used immediately after preparation.

General

The absorption spectra were measured using Shimadzu 2401 equipment at 25 ± 0.1^0C. A Spex fluoromax apparatus was employed for the emission steady-state measurements.

Corrected fluorescence spectra were obtained using the correction file provided by the manufacturer. The path length used in the absorption and emission experiments was 1 cm.

Fluorescence decay data were measured with the time correlated single photon counting technique (Edinburgh Instrument FL-900) with PicoQuant sub-nanosecond Pulsed LED PLS 370 and 450 < 600 ps FWHM. Fluctuations in the pulse and intensity were corrected by making an alternate collection of scattering and sample emission. The quality of the fits was determined by the reduced χ^2. For the best fit χ^2, must be around 1.0.[83]

Acknowledgments

We gratefully acknowledge the financial support for this work by the Consejo Nacional de Investigaciones Científicas y Técnicas (CONICET), Agencia Córdoba Ciencia, Agencia Nacional de Promoción Científica y Técnica and Secretaría de Ciencia y Técnica de la Universidad Nacional de Río Cuarto. N.M.C., J.J.S., F.M. and R.D.F. hold a research position at CONICET. C.C.V. thanks CONICET for a research fellowship.

References

1 I. C. Pintre, S. J. Webb, *Binding and Reactivity at Bilayer Membranes*, Ed.Williams I. H.

2 M. Edidin, *Nat. Rev. Mol. Cell. Biol*., 2003, **4**, 414.

3 G. van Meer, D. R. Voelker, G. W. Feigenson, *Nat. Rev. Mol. Cell. Biol.*, 2008, **9**, 112.

4 A. J. Dzieciol, S. Mann, *Chem. Soc. Rev.*, 2012, **41**,79.

5 N. M. Correa, Z. A. Schelly, H. Zhang, *J. Am. Chem. Soc.* 2000, **122**, 6432.

6 A. Chattopadhyay, S. Mukherjee, *Biochemistry,* 1993, **32**, 3804.

7 C. M. Johnson, S. Baldelli, *Chem. Rev.,* 2014, **114**, 8416.

8 R. R. C. New*, Liposomes. A practical approach*, Ed. Oxford University Press Inc., New York, 1997.

9 M. Kępczyński, K. Nawalani, B. Jachimska, M. Romek, M. Nowakowska, *Coll. and Surf. B: Biointerfaces*. 2006, **49**, 22.

10 J. S. Florez Tabares, M. L. Blas, L. E. Sereno, J. J. Silber, N. M. Correa, P. G. Molina, *Electrochimica Acta.* 2011, **56**, 10231.

11 F. Moyano, P. G. Molina, J. J. Silber, L. Sereno, N. M. Correa, *ChemPhysChem.* 2010, **11**, 236.

12 I. Onyesom, D. A. Lamprou, L. Sygellou, S. K. Owusu-Ware, M. Antonijevic, B. Z. Chowdhry, D. Douroumis, *Mol. Pharm.,* 2013, **10**, 4281.

13 S. Mandal, C. Banerjee, S. Ghosh, J. Kuchlyan, N. Sarkar, *J. Phys. Chem. B*, 2013, **117**, 6957.

14 P. Tanner, P. Baumann, R. Enea, O. Onaca, C. Palivan, W. Meier, *Acc. Chem. Res.*, 2011, **44**, 1039.

15 R. Chandrawati, F. Caruso, *Langmuir,* 2012, **28**, 13798.

16 L. Tavano, R. Muzzalupo, L. Mauro, M. Pellegrino, S. Andó, N. Picci, *Langmuir*, 2013, **29**, 12638.

17 K. Yang, L. Z. Zhu, B. S. Xing, *Environ. Sci. Technol.* 2006, **40**, 4274.

18 A. A. Dar, G. M. Rather, S. Ghosh, A. R. Das, *J. Colloid Interface Sci.* 2008, **322**, 572.

19 Catanionic surfactants, Ed. Specialists Surfactants, Blackie Academic and Professional, Chapman & Hall, London, 1997. 40.

20 B. F. B. Silva, E. F. Marques, Ulf Olsson, *Soft Matter.,* 2011, **7**, 225.

21 B. Abecassis, F. Testard, L. Arleth, S. Hansen, I. Grillo, T. Zemb, *Langmuir* 2007, **23**, 9983.

22 C. C. Villa, F. Moyano, M. Ceolin, J. J. Silber. R. D. Falcone, N. M. Correa, *Chem. Eur. J.* 2012, **18**, 15598.

23 S. Song, Q. Zheng, A. Song, J. Hao, *Langmuir,* 2012, **28**, 219.

24 St. Schmölzer, D. Gräbner, M. Gradzielski, T. Narayanan, *Phys. Rev. Lett.,* 2002, **88**, 258301.

25 X. Li, S. Dong, X. Jia, A. Song, J. Hao, *Chem. Eur. J.,* 2007, **13**, 9495.

26 M. Dubois, V. Lizunov, A. Meister, T. Gulik-Krzywicki, J. M. Verbavatz, E. Perez, J. Zimmerberg, T. Zemb, *Proc. Natl. Acad. Sci.*, 2004, **101**, 15082.

27 J. Hao, W. Liu, G. Xu, L. Zheng, *Langmuir,* 2003, **19**, 10635.

28 H. Li, J. Hao, *J. Phys. Chem. B.* 2008, **112**, 10497.

29 J. Hao, H. Hoffmann, *Curr. Opin. Colloid Interface Sci.* 2004, 9, 279.

30 B. F. B. Silva, E. F. Marques, Ulf Olsson, R. Pons, *Langmuir.* 2010, **26**, 3058.

31 E. W. Kaler, A. K. Murthy, B. Rodriguez, J. A. N. Zasadzinski, *Science* 1989, **245**, 1371.

32 E. F. Marques, O. Regev , A. Khan, B. Lindman. *Adv. Colloid and Interface Sci.* 2003, **100 –102**, 83.

33 G. Salamat, R. Vries, E. W. Kaler. *Langmuir*. 2000, **16**, 102.

34 P. Jokela, B. Jonsson, A. Khan, *J. Phys. Chem.* 1987, **91**, 3291.

35 B. Jonsson, P. Jokela, A. Khan, B. Lindman, A. Sadaghiani. *Langmuir* 1991, **7**, 889.

36 H. Edlund, A. Sadaghiani, A. Khan, *Langmuir* 1997, **13**, 4953.

37 A. Gonzalez-Perez, M. Schmutz, G. Waton, M. J. Romero, M. P. Krafft, *J. Am. Chem. Soc.* 2007, **129**, 756.

38 Y. W.Shen, J. C. Hao, Hoffmann, *Soft Matter* 2007, **3**, 1407.

39 A. Song, S. Dong, X. Jia, J. Hao, W. Liu, T. Liu, *Angew. Chem. Int. Ed.* 2005, **44**, 4018.

40 C. C. Villa, J. J. Silber, N. M. Correa, R. D. Falcone, *ChemPhysChem*, 2014, **15**, 3097.

41 B. F. B. Silva, E. F. Marques, U. Olsson, *Langmuir,* 2008, **24**, 10746.

42 B. F. B. Silva, E. F. Marques, U. Olsson, *J. Phys. Chem. B* 2007, **111**, 13520.

43 T. Welton, *Green Chem.* 2011, **13**, 225.

44 J. P. Hallett, T. Welton, *Chem. Rev.* 2011, **111**, 3508.

45 P. Wasserscheid, W. Keim, *Angew. Chem. Int. Ed.,* 2000, **39**, 3772.

46 T. Welton, *Chem. Rev.,* 1999, **99**, 2071.

47 T. Welton, P. Wasserscheid, *Ionic Liquids in Synthesis*, VCH-Wiley, Weinheim, 2002.

48 T. Welton, *Coordin. Chem. Rev.,* 2004, **248**, 2459.

49 Y. R. Zhao, X. Chen, B. Jing, X. D. Wang, F. Ma, *J. Phys. Chem. B* 2009, **113**, 983.

50 F. Geng, J. Liu, L. Q. Zheng, L. Yu, Z. Li, G. Z. Li, C. H. Tung, *J. Chem. Eng. Data* 2010, **55**, 147.

51 P. Brown, C. Butts, R. Dyer, J. Eastoe, I. Grillo, F. Guittard, S. Rogers, R. Heenan, *Langmuir,* 2011, **27**, 4563.

52 P. Brown, C. P. Butts, J. Eastoe, I. Grillo, C. James, A. Khan, *J. Colloid Interface Sci*. 2013, **395**, 185.

53 P. Brown, C. P. Butts, J. Eastoe, D. Fermin, I. Grillo, H-C. Lee, D. Parker, D. Plana, R. M. Richardson, *Langmuir,* 2012, **28**, 2502.

54 F. Moyano, S. S. Quintana, R. D. Falcone, J. J. Silber, N. Mariano Correa. *J. Phys. Chem. B.* 2009, **113**, 4284.

55 F. M. Agazzi, J. Rodriguez, R. D. Falcone, J. J. Silber, N. M. Correa, *Langmuir* 2013, **29**, 3556.

56 S. S. Quintana, F. Moyano, R. D. Falcone, N. M. Correa. *J. Phys. Chem. B.* 2009, **113**, 6718.

57 F. Moyano, M.A. Biasutti, J.J. Silber, N.M. Correa. *J. Phys. Chem. B*. 2006, **110***,* 11838.

58 F. Moyano, J. J Silber, N. M. Correa, *J. Colloid Interface Sci.,* 2008, **317**, 332.

59 M. Novaira, M. A. Biasutti, J. J Silber, N. M. Correa, N. M. *J. Phys. Chem. B* 2007, **111**, 748.

60 Z. R. Grabowski, K. Rotkiewicz, W. Rettig, *Chem. Rev.* 2003, **103**, 3899.

61 M, Novaira, F. Moyano, M. A. Biasutti, J. J. Silber, N. M. Correa, *Langmuir,* 2008, **24**, 4637.

62 J. Barucha-Kraszewska, S. Kraszewski, P. Jurkiewicz, C. Ramseyer, M. Hof, *Biochim. Biophys. Acta,* 2010, **1798**, 1724.

63 E. A. Lissi, E. B. Abuin, M. A. Rubio, A. Cerón, *Langmuir* 2000, **16**, 178.

64 W. K. Nitschke, C. C. Vequi-Suplicy, K. Coutinho, H. Stassen, *J. Phys. Chem. B* 2012, **116**, 2713.

65 R. Adhikary, C. A. Barnes, J. W. Petrich, *J. Phys. Chem. B,* 2009, **113**, 11999.

66 K. K. Karukstis, C. A. Zieleniuk, M. J. Fox, *Langmuir* 2003, **19**, 10054.

67 E. K. Krasnowska, L. A. Bagatolli, E. Gratton, T. Parasassi, *Biochim. Biophys. Acta* 2001, **1511**, 330.

68 B. Mennucci, M. Caricato, F. Ingrosso, C. Cappelli, R. Cammi, J. Tomasi, G. Scalmani, M. J. Frisch, *J. Phys. Chem. B,* 2007, **112**, 414.

69 L. Cwiklik, A. J. A. Aquino, M. Vazdar, P. Jurkiewicz, J. Pittner, M. Hof, H. Lischka, *J. Phys. Chem. A,* 2011, **115**, 11428.

70 B. Sengupta, J. Guharay, P. K. Sengupta, *Spectrochim. Acta, Part A,* 2000, **56**, 1433.

71 A. Balter, W. Nowak, W. Pawełkiewicz, A. Kowalczyk, *Chem. Phys. Lett.,* 1988, **143**, 565.

72 J. Catalan, P. Perez, J. Laynez, F. G. Blanco, *J. Fluoresc.* 1991, **1**, 215.

73 F. M. Cerezo, S. C. Rocafort, P. S. Sierra, F. García-Blanco, C. D. Oliva, J. C. Sierra, *Helv. Chim. Acta,* 2001, **84**, 3306.

74 J. Kim, M. Lee, *J. Phys. Chem. A*, 1999, **103**, 3378.

75 J. R. Lakowicz, *Principles of Fluorescence Spectroscopy*, 2nd Ed., Kluwer Academic, New York, New York. 1999.

76 J. Milhaud, *Biochim. Biophys. Acta,* 2004, **1663**, 19.

77 A. Chattopadhyay, *Chem. Phys. Lipids.,* 2003, **122**, 3.

78 A. Chattopadhyay, S. Murkherjee, H. Raghuraman, *J. Phys. Chem. B,* 2002, **106**, 13002.

79 A. Chattopadhyay, S. Murkherjee, *Biochemistry,* 1994, **33**, 5089-5097.

80 P. L-G. Chong, *Biochemistry,* 1988, **27**, 399.

81 M. Hof, P. Lianos, A. Laschewsky, *Langmuir,* 1997, **13**, 2181.

82 K. Lunkenheimer, A. Laschewsky, *Prog. Colloid Polym. Sci.* 1992, **89**, 239.

83 D. V. O'Connor, D. Phillips, *Time-Correlated Single Photon Counting*; Academic Press: New York, 1983; Chapter 6.

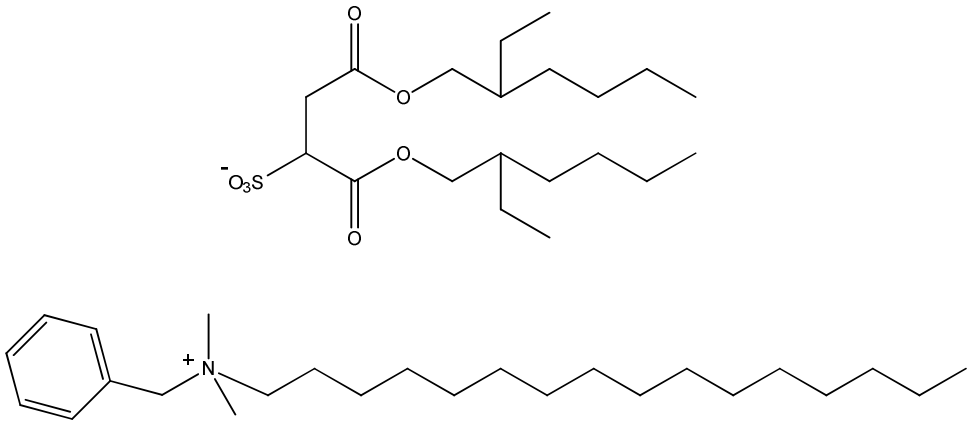

AOT-BHD

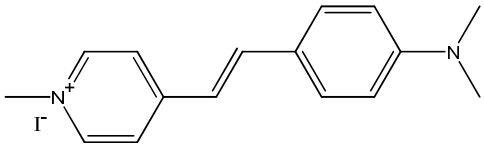

HC

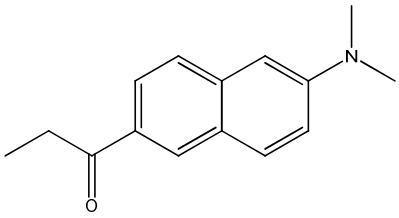

PRODAN

Scheme 1. Molecular structures of the catanionic surfactant AOT-BHD, HC and PRODAN.

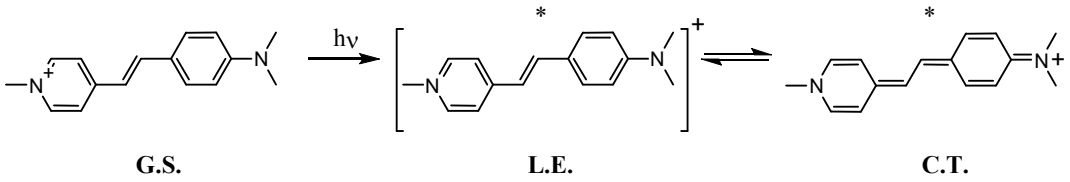

Scheme 2. Representative HC structures as it is explained in the text.

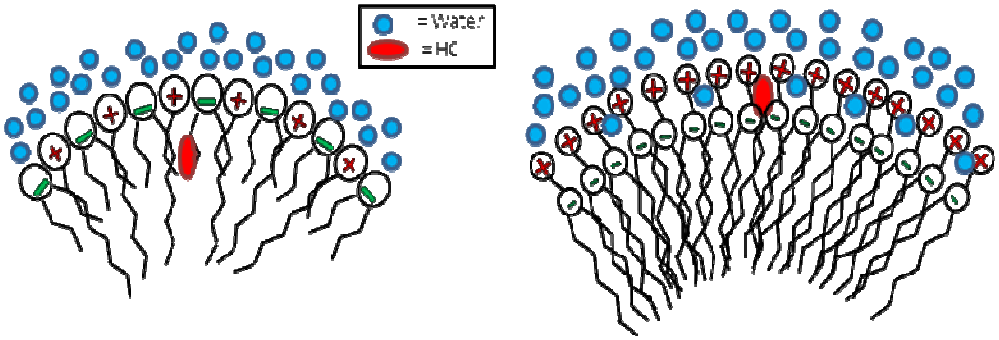

a **b**

Scheme 3. Schematic representation of HC location into the vesicles of: (a) AOT-BHD and (b) DOPC.

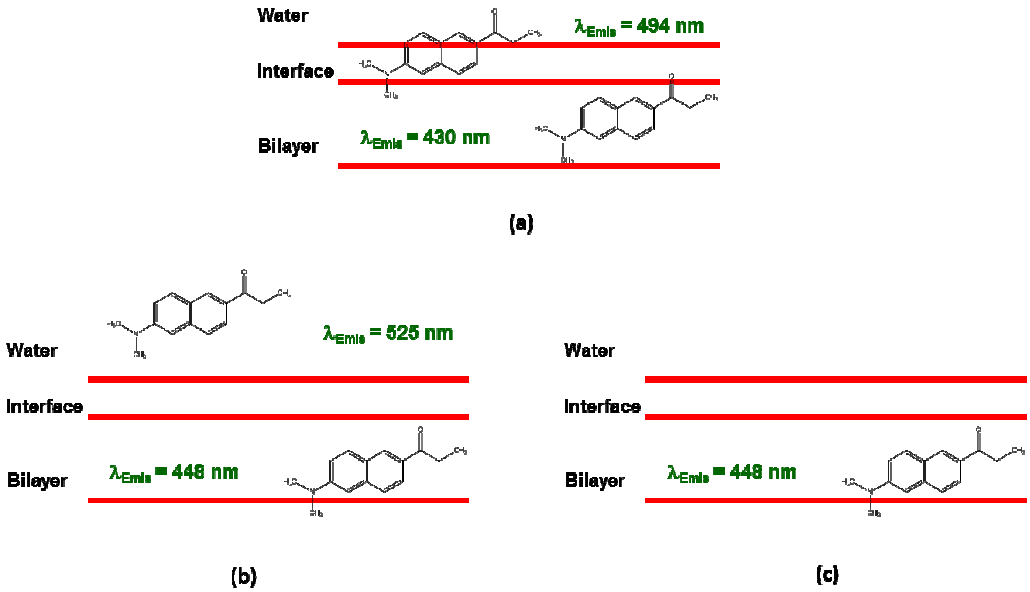

Scheme 4. Schematic representation of PRODAN location into the vesicles of: (a) DOPC at [DOPC] = 1 mg/mL; (b) AOT-BHD at [AOT-BHD] < 0.5 mg/mL and (c) AOT-BHD at [AOT-BHD] > 2 mg/mL.

Table 1. Fluorescence lifetime values (τ, ns) of HC in AOT-BHD vesicles at different emission wavelengths. λ_{exc} = 450 nm. [AOT-BHD] = 2 mg/mL. [HC] = 1 x 10^{-5} M.

λ_{em} (nm)	τ	χ^2
585	1.5 ± 0.2	1.07
600	1.7 ± 0.1	1.18
615	1.8 ± 0.1	1.22
630	1.9 ± 0.1	1.20
645	2.1 ± 0.2	1.25

Table 2. Fluorescence lifetime values (τ, ns)[a] of PRODAN in water and in AOT-BHD vesicles. [PRODAN] = 5 x 10^{-6} M. λ_{exc} = 378 nm. λ_{em} = 525 nm.

[AOT-BHD] (mg/mL)	**τ_1**	**τ_2**	**χ^2**
0	0.71 ± 0.04 (59.6 %)	2.12 ± 0.09 (40.4 %)	1.13
0.5	0.69 ± 0.03 (39.1 %)	3.82 ± 0.08 (60.9 %)	1.12
1	0.70 ± 0.02 (9.4 %)	3.85 ± 0.05 (90.6 %)	1.15
2	-	4.17 ± 0.02 (100 %)	1.14
3	-	4.01 ± 0.05 (100 %)	1.31

[a] The values in parentheses are the contribution of the species obtained from the fit.

Table 3. Partition constant (K_p) values obtained for HC and PRODAN in AOT-BHD and DOPC vesicles.

HC	
AOT-BHD[a]	**DOPC**[b]
18.1 ± 0.1 mL/mg (18900 ± 378 M^{-1})	2.35 ± 0.13 mL/mg (1850 ± 400 M^{-1})
PRODAN	
AOT-BHD[a]	**DOPC**[c]
25 ± 2 mL/mg (19800 ± 990 M^{-1})	16 ± 2 mL/mg (12900 ± 1300 M^{-1})

[a] Values calculated using equation S5 from the supporting information section. [b] K_p value from reference 58. [c] K_p value from reference 57.

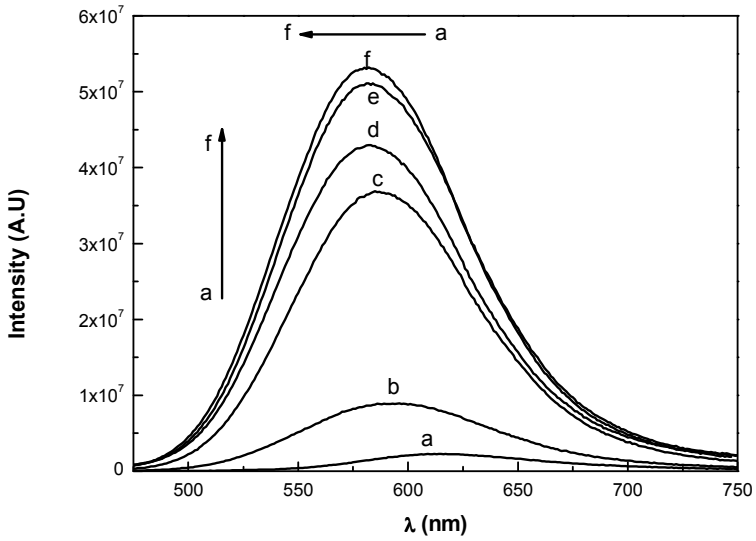

Figure 1. Emission spectra of HC in AOT-BHD unilamellar vesicles varying [AOT-BHD]. [AOT-BHD]: a) 0 mg/mL, b) 0.1 mg/mL, c) 0.5 mg/mL, d) 1 mg/mL, e) 3 mg/mL, f) 5 mg/mL, λ_{exc} = 450 nm. [HC] = 1 x 10^{-5} M.

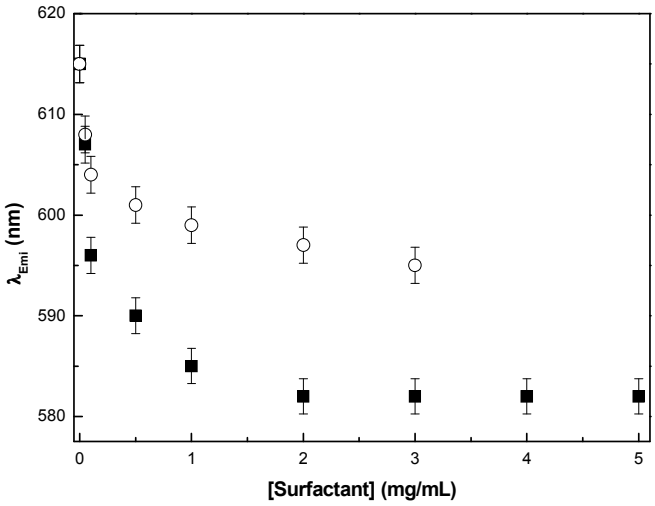

Figure 2. Variation of HC emission wavelength maxima (λ_{em}) as a function of [surfactant] in AOT-BHD (■) and DOPC (○) vesicles. λ_{exc} = 450 nm. [HC] = 1 x 10^{-5} M. DOPC values taken from reference 58.

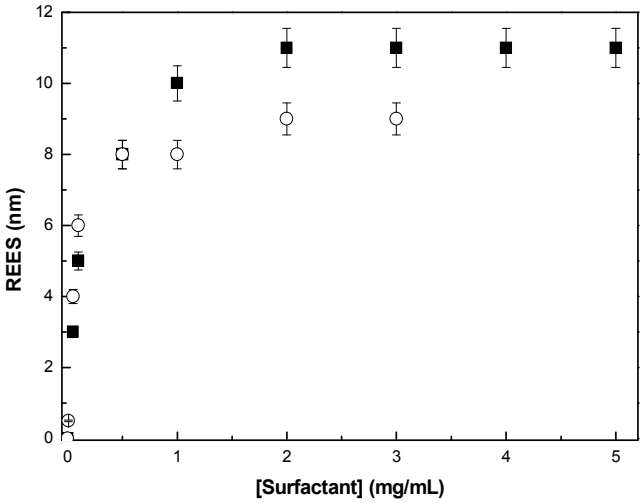

Figure 3. REES values of HC in AOT-BHD (■) and DOPC (○) vesicles, increasing the [surfactant]. REES = $\Delta\lambda_{em}$ = ($\lambda_{em\ (exc\ 510\ nm)}$ - ($\lambda_{em\ (exc\ 450\ nm)}$). [HC] = 1 x 10^{-5} M. DOPC values taken from reference 58.

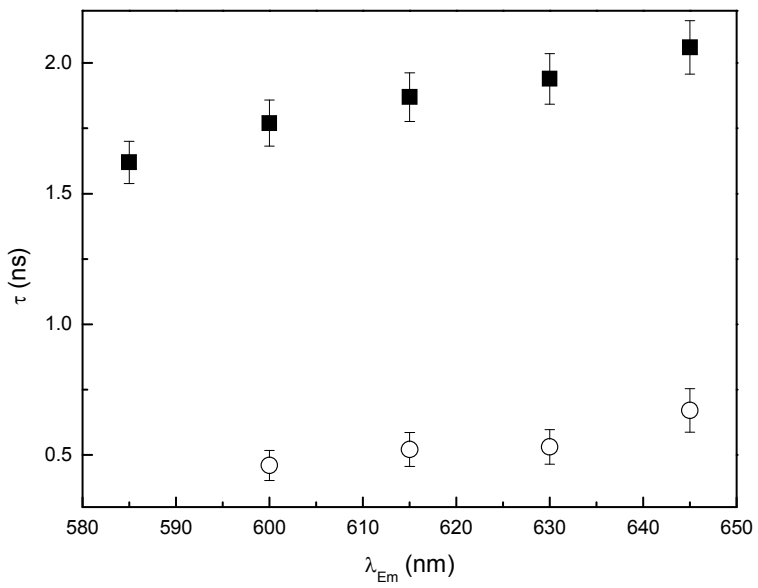

Figure 4. Fluorescence lifetime (τ) values as a function of the emission wavelength of HC in (■) AOT-BHD and (○) DOPC vesicles. [HC] = 1 x 10^{-5} M. DOPC values taken from reference 58. λ_{exc} = 450 nm.

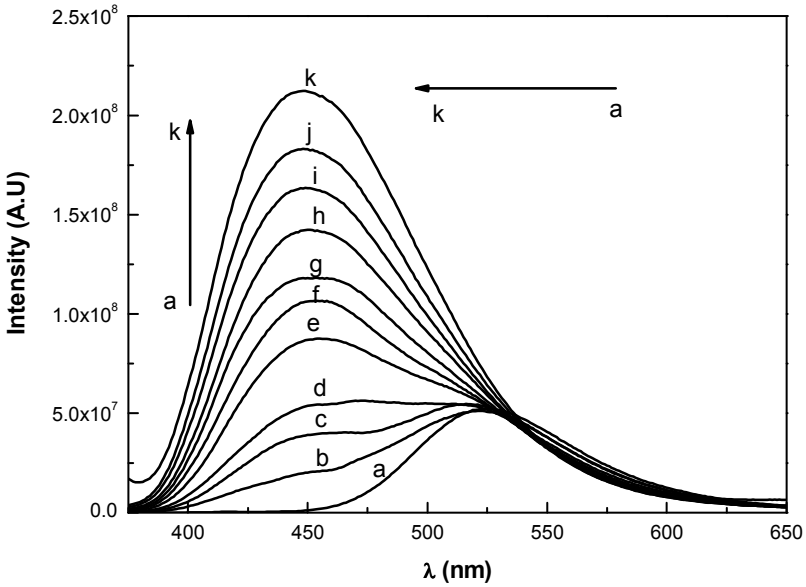

Figure 5. Emission spectra of PRODAN in AOT-BHD unilamellar vesicles varying [AOT-BHD]. [AOT-BHD]: a) 0 mg/mL, b) 0.05 mg/mL, c) 0.1 mg/mL, d) 0.25 mg/mL, e) 0.5 mg/mL, f) 0.75 mg/mL, g) 1 mg/mL, h) 1.5 mg/mL, i) 2 mg/mL, j) 3 mg/mL, k) 5 mg/mL. λ_{exc} = 350 nm. [PRODAN] = 5 x 10^{-6} M.

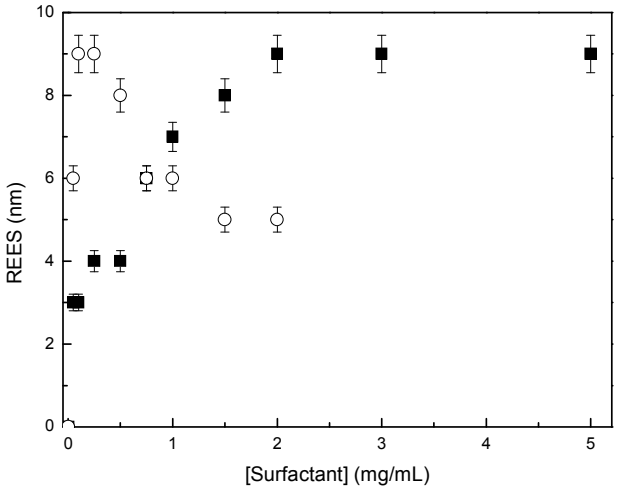

Figure 6. REES values of PRODAN in (■) AOT-BHD and (○) DOPC vesicles, increasing the [surfactant]. REES = $\Delta\lambda_{em}$ = ($\lambda_{em\ (exc\ 410nm)}$ - ($\lambda_{em\ (exc\ 350nm)}$). [PRODAN] = 5 x 10^{-6} M. DOPC values taken from reference 57. λ_{exc} = 350 nm.

TOC

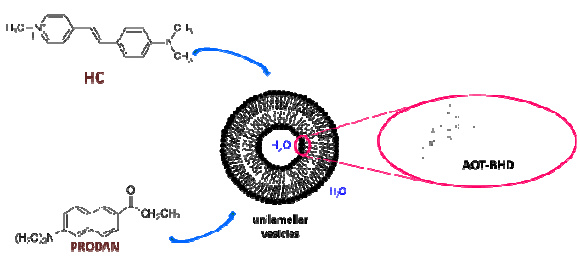

AOT-BHD vesicles present a bilayer completely different to the traditional DOPC one, with low polarity, high viscosity and more electron donor capacity.